Catalysis Today 143 (2009) 45–50

Contents lists available at ScienceDirect

Catalysis Today

journal homepage: www.elsevier.com/locate/cattod

Water-gas shift activity of Cu surfaces and Cu nanoparticles supported on metal oxides

J.A. Rodriguez [a,*], P. Liu [a], X. Wang [a], W. Wen [a], J. Hanson [a], J. Hrbek [a], M. Pérez [b], J. Evans [b]

[a] Chemistry Department, Brookhaven National Laboratory, Upton, NY 11973, USA
[b] Facultad de Ciencias, Universidad Central de Venezuela, Caracas 1020-A, Venezuela

ARTICLE INFO

Article history:
Available online 18 September 2008

Keywords:
Copper
Magnesium oxide
Metal oxides
Carbon monoxide
Hydrogen production
Water
Water-gas shift
CO oxidation

ABSTRACT

Oxide supported Cu catalysts show significant activity for the water-gas shift reaction (WGS, $CO + H_2O \rightarrow H_2 + CO_2$) but their performance is not fully understood and is highly dependent on the synthesis conditions or the nature of the oxide support. This article describes a series of new studies examining the water-gas shift activity of Cu/MgO(1 0 0) surfaces and compares it to the activities found for pure copper systems, Cu nanoparticles in contact with well-defined surfaces of TiO_2, ZnO, MoO_2 and CeO_2, and Cu cations present in mixed-metal oxides. Catalytic tests performed over $CuFe_2O_4$, $Ce_{1-x}Cu_xO_2$ or $CuMoO_4$ show significant WGS activity only when the Cu cations in the mixed-metal oxide are reduced to metallic copper. Thus, Cu nanoparticles were deposited on different oxide surfaces and their WGS activity was measured in a batch reactor (P_{CO} = 20 Torr; P_{H_2O} = 10 Torr; T = 575–650 K). The WGS activity of the Cu nanoparticles supported on MgO(1 0 0) was 2–3 times larger than that of Cu(1 0 0). Even better WGS catalysts were obtained when Cu was deposited on CeO_2(1 1 1) or TiO_2(1 1 0). An apparent activation energy of 13.8 kcal/mol was found for the WGS on Cu/MgO(1 0 0). This is smaller than the value of 15.2 kcal/mol observed on Cu(1 0 0), and substantially larger than the values of 7–9 kcal/mol seen for the apparent activation energies of the Cu/CeO_2(1 1 1) and Cu/TiO_2(1 1 0) catalysts. Post-reaction surface characterization pointed to the lack of O vacancies in the Cu/MgO(1 0 0) catalysts. This is in contrast to results found for Cu/CeO_2(1 1 1) and Cu/TiO_2(1 1 0), where the oxide support exhibits a significant concentration of O vacancies as a consequence of the WGS reaction. The oxygen vacancies present in Cu/CeO_2(1 1 1) and Cu/TiO_2(1 1 0) help in the dissociation of the water molecule and reduce the apparent activation energy for the WGS process. Such a phenomenon cannot occur on the Cu/MgO(0 0 1) catalysts, and the main steps of the WGS probably take place on the Cu nanoparticles.

1. Introduction

The water-gas shift (WGS, $CO + H_2O \rightarrow CO_2 + H_2$) is an important reaction used in the chemical industry for the production of clean H_2. Currently, the primary source of hydrogen is based on the steam reforming of hydrocarbons: $C_nH_m + nH_2O \rightarrow nCO + (n - m/2)H_2$. The reformed fuel contains 1–10% of CO, which degrades the performance of the Pt electrode utilized in fuel cell systems. The water-gas shift reaction is critical for providing clean hydrogen [1–5].

At the present time, mixtures of Fe–Cr and Zn–Al–Cu oxides are the commercially used catalysts for the water-gas shift reaction at temperatures between 350–500 and 180–250 °C, respectively. However, these oxide catalysts are pyrophoric and normally require lengthy and complex activation steps before usage [1]. Consequently better catalysts are being sought [5]. Oxide supported Cu catalysts show significant water-gas shift activity but their performance is not fully understood and is highly dependent on the synthesis conditions or the nature of the oxide support [1–5]. Either metallic Cu or Cu^{1+} cations have been proposed as the active sites for the WGS reaction [1]. The oxide component in the catalysts may not be a simple spectator and play a direct role in the dissociation of water or in the generation of key intermediates (formates, carbonates, formyls, etc.) [2,5]. In principle, the active sites for the WGS could be located on the perimeter of the copper-oxide interface.

This article describes a series of new studies examining the water-gas shift activity of Cu/MgO(1 0 0) surfaces and compares it to the activities found for pure copper systems [4,6–8], Cu nanoparticles in contact with well-defined surfaces of TiO_2, ZnO, MoO_2 and CeO_2 [4,9–11], and Cu cations present in mixed-metal oxides [12,13]. Experiments performed in our laboratory for the water-gas shift on $Ce_{1-x}Cu_xO_2$ or $CuMoO_4$ have shown significant catalytic activity only when the Cu cations in the mixed-metal oxide are reduced to metallic copper [12,13]. Recently, we have performed similar experiments over $CuFe_2O_4$ and again the results

* Corresponding author. Tel.: +1 631 344 2246; fax: +1 631 344 5815.
E-mail address: rodrigez@bnl.gov (J.A. Rodriguez).

0920-5861/$ – see front matter © 2008 Elsevier B.V. All rights reserved.
doi:10.1016/j.cattod.2008.08.022

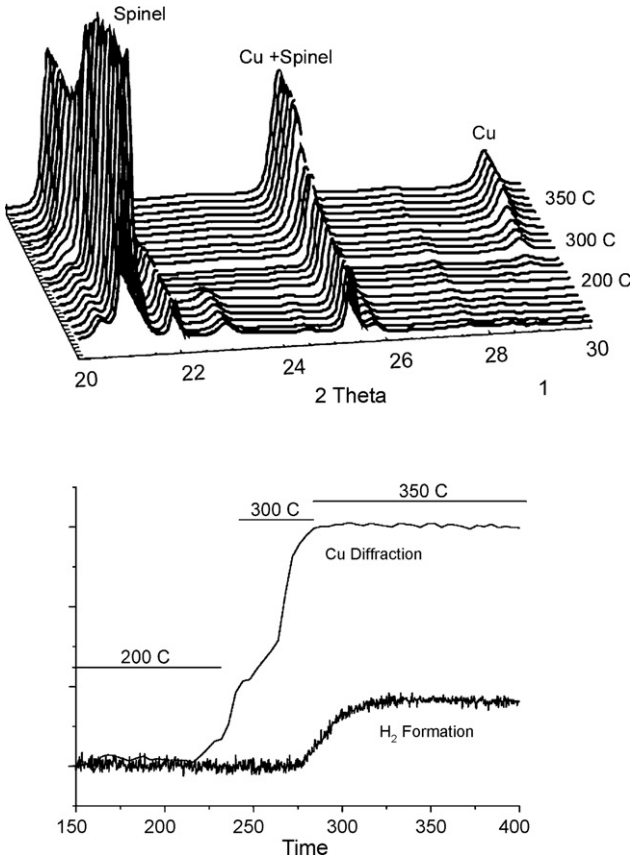

Fig. 1. Top: X-ray diffraction patterns collected *in situ* during the WGS reaction on $CuFe_2O_4$ at different temperatures. The $CuFe_2O_4$ spinel undergoes partial reduction to yield metallic Cu on an oxide matrix. Bottom: Evolution of the signal for metallic Cu (measured by X-ray diffraction) and H_2 generation (measured by mass spectrometry) as a function of temperature and time (in min). In these experiments ~3 mg of the $CuFe_2O_4$ spinel were loaded in a microreactor under a flow of CO/H_2O [12,13] and then the sample temperature was held at the indicated values.

of *in situ* time-resolved XRD show a correlation between the generation of metallic copper ($Cu^{2+} \rightarrow Cu^0$) and the appearance of catalytic activity, see Fig. 1. On the basis of these results, the first part of the article is devoted to review what is known for the WGS on pure copper surfaces and nanoparticles. Previous studies examining the WGS on well-defined surfaces have focused on the (1 1 1), (1 1 0) and (1 0 0) faces of copper [4,8], and on systems containing nanoparticles of copper dispersed on ZnO(0 0 0 $\bar{1}$) [4], CeO_2(1 1 1) [4], TiO_2(1 1 0) [10] and polycrystalline MoO_2 [9]. Here, the Cu is deposited on a highly ionic oxide support: MgO. The model Cu/MgO(0 0 1) catalysts were prepared and characterized in an ultra-high vacuum chamber and their catalytic activity was tested in an attached high-pressure reactor [9,11]. This approach has proved to be very useful for studying the kinetics and mechanism of the WGS reaction on copper surfaces [4,8,14,15], and to establish patterns of reactivity on copper/oxide surfaces as a function of admetal coverage [4,9]. In this work we go one step further and the data for Cu/MgO(0 0 1) allows us to examine the role on the oxide in the WGS reaction.

2. Experimental and theoretical methods

2.1. Water-gas shift studies on Cu/MgO(0 0 1) and extended copper surfaces

Most experiments were performed in an ultrahigh-vacuum (UHV) chamber that has attached a high-pressure cell or batch reactor [4,9]. The sample could be transferred between the reactor and vacuum chamber without exposure to air. The UHV chamber (base pressure $\sim 5 \times 10^{-10}$ Torr) was equipped with instrumentation for X-ray photoelectron spectroscopy (XPS), low-energy electron diffraction (LEED), ion scattering spectroscopy (ISS), and thermal-desorption mass spectroscopy (TDS).

Most WGS catalysts contain ZnO, CeO_2 or TiO_2 as supports [4,5,10,16]. Here, the Cu was deposited on a highly ionic oxide support: MgO. Ultrathin films (30–40 Å in thickness) of MgO(1 0 0) were grown on a Mo(1 0 0) crystal [17,18]. In short, high-purity (99.999%) Mg was vapour deposited on Mo(1 0 0) at 500–600 K in a background O_2 pressure of $\sim 2 \times 10^{-6}$ Torr. This was followed by heating to 1200 K in 1×10^{-6} Torr of O_2 [17–19]. Such a procedure leads to the formation of well-ordered films of MgO(1 0 0) on the Mo(1 0 0) substrate that can be studied with XPS without problems of charging [17–19]. Cu was vapour deposited on the MgO(1 0 0) surface at room temperature [19]. The evaporation of copper was achieved by heating a W filament wrapped with an ultra-pure (99.999%) Cu wire. The atomic flux from this metal doser was calibrated using the methodology described in Ref. [19]: comparison of Cu-thermal desorption spectra from Cu/MgO(1 0 0)/Mo(1 0 0) and Cu/Mo(1 0 0). A dose of one monolayer (ML) of the admetal corresponds to a coverage equal to the first layer of Cu on Mo(1 0 0). ISS indicates that Cu grows on MgO(1 0 0) forming three-dimensional (3D) islands as seen on CeO_2(1 1 1), ZnO(0 0 0 $\bar{1}$) or TiO_2(1 1 0). After each experiment with the Cu/MgO(1 0 0)/Mo(1 0 0) surfaces, the Mo(1 0 0) substrate was cleaned by e-beam heating it to 2200 K.

In the kinetic measurements the sample was transferred to the batch reactor at ~300 K, then the reactant gases were introduced (20 Torr of CO and 10 Torr of H_2O) and the sample was rapidly heated to the reaction temperature (575, 600, 625 or 650 K). The CO gas was cleaned of any metal carbonyl impurity by passing it through purification traps. Product yields were analyzed by a gas chromatograph [4,9]. The amount of molecules produced was normalized by the active area exposed by the sample. The sample holder was passivated by extensive sulphur poisoning (exposure to H_2S) and has no catalytic activity. In our reactor a steady-state regime for the production of H_2 and CO_2 was reached after 2–3 min of reaction time. The kinetic experiments were done in the limit of low conversion (<5%).

2.2. Density-functional calculations

The unrestricted density-functional (DF) calculations were performed with the DMol^3 code, using effective core potentials, a numerical basis set, and the GGA-PW91 description of the exchange and correlation functionals [6,20]. Transition states here were identified using the combination of synchronous transit methods and eigenvector following, and verified by the presence of a single imaginary frequency from a sequential vibrational frequency analysis. Cu(1 0 0) was modelled using four-layer slabs [21]. During the DF calculations the geometries of the top two layers of the slabs and the Cu nanoparticles were fully relaxed.

3. Results and discussion

3.1. The water-gas shift reaction on copper surfaces and nanoparticles

The top of Fig. 2 displays the accumulation of CO_2 and H_2 as a function of time for the WGS reaction over clean Cu(1 0 0) between 575 and 650 K for a reactant mixture of 20 Torr of CO and 10 Torr of H_2O. In general, we found that the amounts of H_2 and CO_2 formed increase linearly with time. The reaction rapidly reached steady-state and operated in the limit of low conversion (<5%). Post-

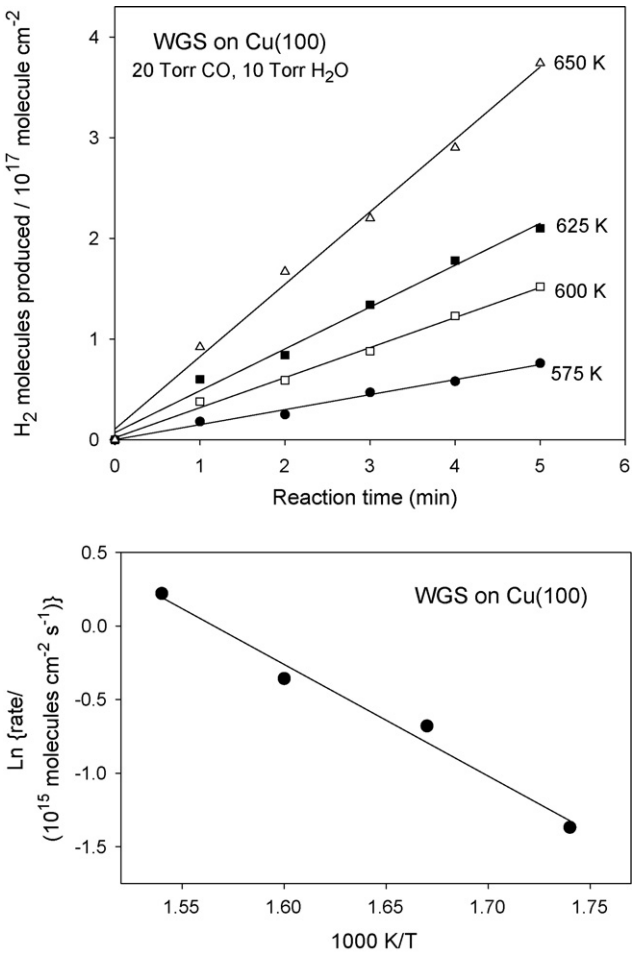

Fig. 2. Top: Production of H_2 through the WGS on a Cu(1 0 0) catalyst. At each temperature the copper surface was exposed to a mixture of 20 Torr of CO and 10 Torr of H_2O for 5 min. Bottom: The WGS reaction rate *versus* temperature, in Arrhenius form.

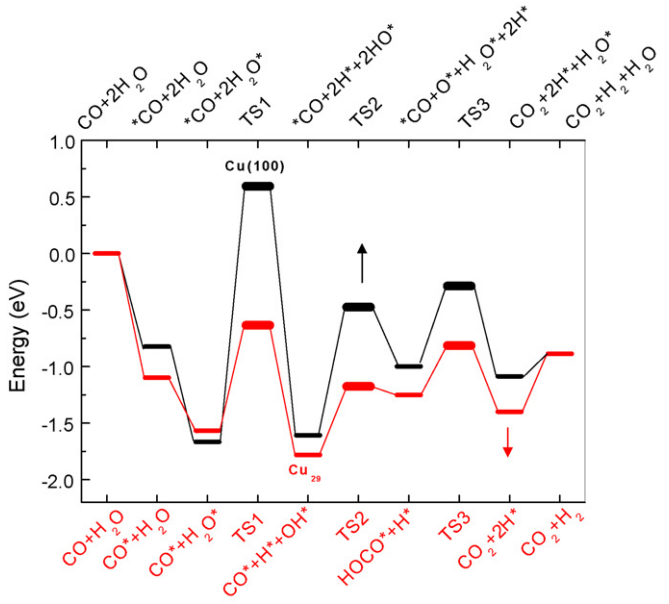

Fig. 3. Calculated potential energy diagram for the WGS on Cu(1 0 0) and on a Cu_{29} nanoparticle. The symbols along the top refer to Cu(1 0 0), while the symbols along the bottom are for Cu_{29}. The zero energy is taken as the sum of the energies of the bare surface or nanoparticle, gas-phase water, and carbon monoxide [6]. "TS" is used to denote transition states.

reaction surface analysis with XPS showed a small amount of carbon on the surface, and no clear traces for carbonate or formate species. These results for the WGS on the Cu(1 0 0) surface are in good agreement with data previously reported for the WGS on Cu(1 1 1) and Cu(1 1 0) [8,22]. In the bottom of Fig. 2 is shown the corresponding Arrhenius plot for the WGS on Cu(1 0 0). The apparent activation energy given by the slope of the Arrhenius plot is 15.2 kcal/mol. It is somewhat smaller than the value of 17 kcal/mol reported for the WGS on a Cu(1 1 1) surface [8,22]. We found a even smaller apparent activation energy of 13.7 kcal/mol when the WGS reaction was performed over a rough Cu foil.

To date, two main reaction mechanisms have been proposed for the WGS reaction on metal/oxide surfaces. One is a redox mechanism [8,23–26], where CO reacts with an oxygen atom coming from water dissociation or the oxide support to form CO_2. The other is an associative mechanism [5,27–29] where the main reaction intermediates are species such as formate, carbonate, or carboxyl, produced by reaction of CO with terminal hydroxyl groups present in the surface of the catalyst. To clarify several of these issues, density functional theory (DFT) was employed to investigate the WGS on Cu(1 0 0) and Cu(1 1 1) surfaces [6,7].

The full energy profile for the WGS on a Cu(1 0 0) surface, including kinetic barriers, is shown in Fig. 3 [6]. The energies are expressed with respect to the clean surface, a free CO molecule and two H_2O molecules in the gas phase. The adsorption configurations for the reactants, intermediates and transition states (TS) involved in this process are displayed in Fig. 4. As shown, CO adsorbs on fourfold hollow sites of Cu, and the binding energy is ~0.80 eV. A substantial adsorption energy is also observed for H_2O on top of Cu (Fig. 3). The dissociation of water is the most difficult step in the WGS reaction with an activation barrier of the order of ~1 eV. Similar results have also been found for Cu(1 1 0) and Cu(1 1 1) [7,30]. According to the DFT calculations [6], the formation of formate on Cu(1 0 0) should be a reaction very unlikely ($HO^* + CO^* \rightarrow HOOC^*$, ΔE = +2.56 eV), and in contrast the dissociation of *OH and the formation of a carboxyl, $HO^* + CO^* \rightarrow OCOH^*$, are much more facile [6]. Furthermore, the adsorbed carboxyl groups are not stable on Cu(1 0 0) and easily decomposes into OH^* and CO^* (i.e. no H^* and $CO_2{}^*$ formation) [6]. Thus, in the case of Cu(1 0 0), the redox mechanism should be preferred with water dissociation as the rate limiting step [6]. This is consistent with experimental measurements [4,8], which show no significant signal for adsorbed HCOO or CO_x species after performing the WGS on periodic copper surfaces. Additional evidence in support of a redox mechanism comes from experiments in which the rate of CO_2 dissociation to $CO + O^*$ is essentially equal to the rate of the reverse WGS on Cu(1 0 0) at the same temperature and CO_2 pressure, when first-order in CO_2 [8].

Fig. 3 also displays the energy profile for the WGS on a Cu_{29} nanoparticle. Cu_{29} exhibits a pyramidal structure formed by the interconnection of (1 1 1) and (1 0 0) faces of the bulk metals, see Fig. 4. This type of nanoparticle has been observed on CeO_2(1 1 1) with scanning tunneling microscopy [4]. It has three layers (containing 16, 9 and 4 metal atoms) that expose different types of adsorption sites with a large degree of fluxionality [4,6,31]. Thus, Cu_{29} can be taken as a reasonable model for unsupported nanocatalysts. According to DFT calculations [6], Cu_{29} is more active for the WGS than Cu(1 0 0), Cu(1 1 0) or Cu(1 1 1). In Fig. 3, Cu_{29} binds CO better and dissociates water easier than Cu(1 0 0). On Cu_{29}, the WGS probably involves the formation of a HOCO intermediate which precedes the generation of CO_2 and H_2 [6], but

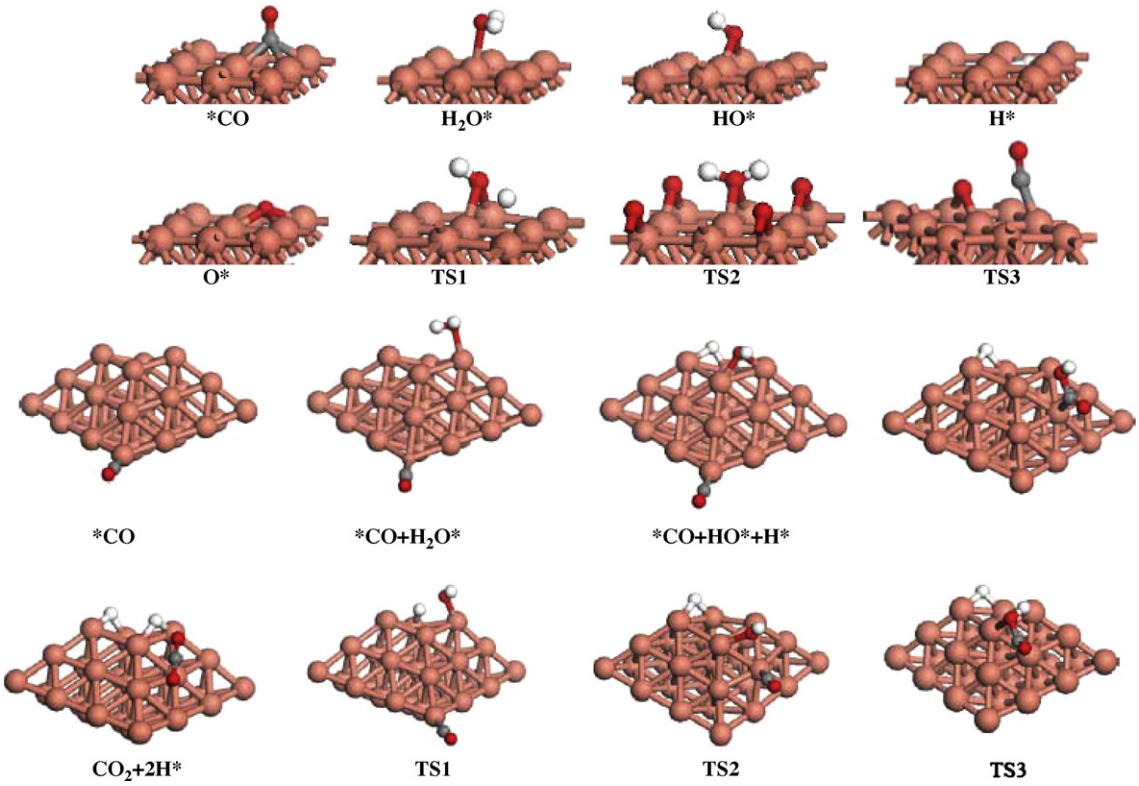

Fig. 4. Calculated structures for intermediates and transition states (TS) involved in the WGS reaction on a Cu(1 0 0) surface and on a Cu_{29} nanoparticle.

on the nanoparticle the dissociation of water is the most difficult step as on the periodic surface. In the next section, we will see that an oxide support can enhance the rate of the WGS reaction by facilitating the dissociation of water.

3.2. Water-gas shift reaction on well-defined copper/oxide surfaces

Previous studies have examined the WGS reaction on model catalysts that consist of copper nanoparticles dispersed on oxide surfaces which have a moderate degree of ionicity: ZnO(0 0 0 $\bar{1}$) [4], CeO_2(1 1 1) [4], TiO_2(1 1 0) [10], and polycrystalline MoO_2 [9]. In this work, we will investigate the behavior of Cu on a highly ionic MgO(1 0 0) surface and compare it to those previously observed for other copper/oxide systems. Fig. 5 shows the WGS activity of model Cu/MgO(1 0 0) catalysts as a function of admetal coverage. The clean MgO(1 0 0) surface displayed no activity for the WGS under the reaction conditions investigated here. Upon adding Cu to MgO(1 0 0), there is a continuous increase in the catalytic activity until a maximum is reached at coverages of 0.4–0.6 ML. After this point, the production of H_2 and CO_2 starts to decrease. This trend can be attributed to a decrease in catalytic activity when the Cu particle size becomes very large [4]. A similar phenomenon has

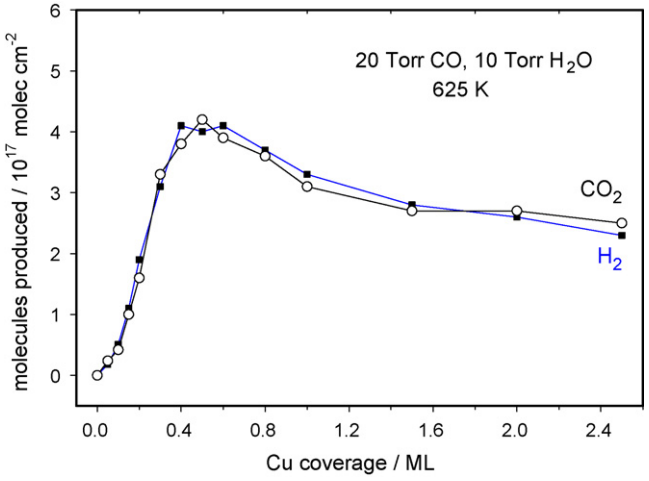

Fig. 5. WGS activity of model Cu/MgO(0 0 1) catalysts as a function of admetal coverage. Each surface was exposed to a mixture of 20 Torr of CO and 10 Torr of H_2O at 625 K for 5 min. Steady-state was reached 2–3 min after introducing the gases in the batch reactor.

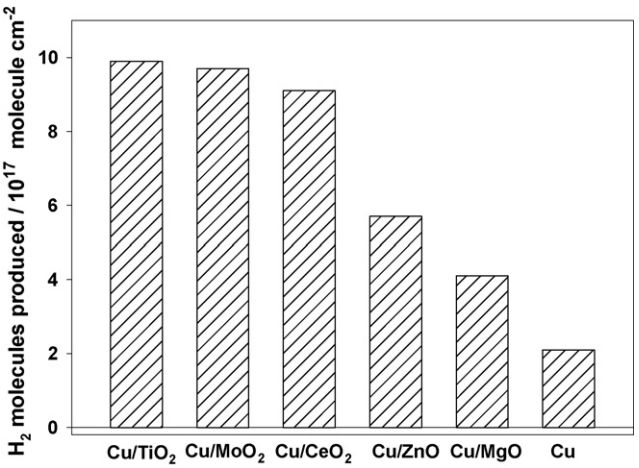

Fig. 6. H_2 produced under similar conditions (20 Torr of CO, 10 Torr of H_2O, 625 K, 5 min) on Cu(1 0 0) and on 0.5 ML of Cu supported over MgO(0 0 1), ZnO(0 0 0 $\bar{1}$) [4], CeO_2(1 1 1) [4], TiO_2(1 1 0) [10] and polycrystalline MoO_2 [9].

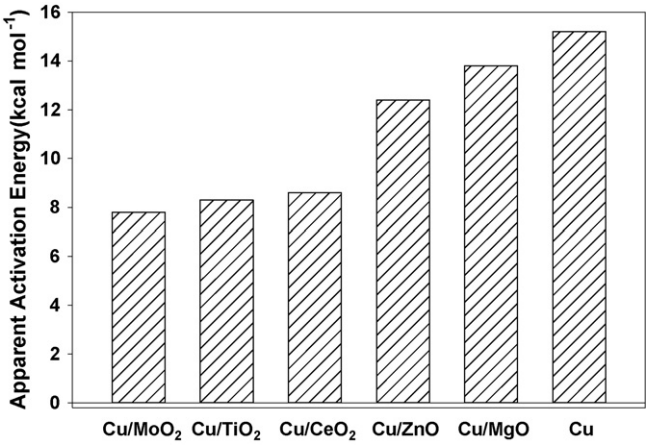

Fig. 7. Apparent activation energies observed for the WGS over 0.5 ML of Cu deposited on MgO(0 0 1), ZnO(0 0 0 $\bar{1}$) [4], CeO_2(1 1 1) [4], TiO_2(1 1 0) [10] and polycrystalline MoO_2 [9]. P_{CO} = 20 Torr, P_{H_2O} = 10 Torr. For comparison, we also include the apparent activation energy found for Cu(1 0 0).

been seen for copper dispersed on other well-defined oxide surfaces [4,9,10].

Fig. 6 compares the amount of H_2 produced under similar conditions (20 Torr of CO, 10 Torr of H_2O, 625 K, 5 min) on Cu(1 0 0) and on 0.5 ML of Cu supported over MgO(1 0 0), ZnO(0 0 0 $\bar{1}$) [4], CeO_2(1 1 1) [4], TiO_2(1 1 0) [10], and polycrystalline MoO_2 [9]. The deposition of Cu nanoparticles on MgO(1 0 0) produces a catalyst that is more active than the Cu(1 0 0) surface. However, an even better catalyst is obtained when the Cu nanoparticles are supported on CeO_2 or MoO_2. These oxides are also better supports than ZnO, which is an oxide support frequently used in commercial catalysts for the WGS [5].

Fig. 7 displays the apparent activation energies observed for the WGS on Cu(1 0 0) and on 0.5 ML of Cu supported over MgO(1 0 0), ZnO(0 0 0 $\bar{1}$) [4], CeO_2(1 1 1) [4], TiO_2(1 1 0) [10], and polycrystalline MoO_2 [9]. All the reported values were obtained from Arrhenius plots that contained reaction rates measured at 575, 600, 625 and 650 K under steady state conditions at P_{CO} = 20 Torr and P_{H_2O} = 10 Torr. An apparent activation energy of 13.8 kcal/mol was found for the Cu/MgO(1 0 0) catalyst. This is smaller than the value of 15.2 kcal/mol observed for Cu(1 0 0), comparable to the value of 13.7 kcal/mol seen for a rough Cu foil, and substantially larger than the values of 7–9 kcal/mol seen for the apparent activation energies of the best WGS catalysts.

The kinetic data in Figs. 5–7 were collected using a reaction cell attached to an ultra-high vacuum chamber for surface characterization. The gases were pumped out from the reaction cell and the surfaces were post-characterized using standard XPS. In the C 1s region we found the typical peaks for adsorbed formate- or carbonate-like species proposed as intermediates in the WGS reaction [5]. Such species were not seen on Cu(1 0 0) or on a rough Cu foil, and are formed on Cu/MgO(0 0 1) or other copper/oxide systems [4,9,10] due to their high stability when bonded to oxide compounds [15]. The adsorbed formate- or carbonate-like species could be mere spectators and not be real intermediates in the WGS process [5,15,32], because they interact too strongly with the catalyst surface [15]. In the post-reaction XPS, the Cu 2p core-level and L_3VV Auger transition indicated that Cu remained in a metallic state [33]. There was attenuation in the Mg and O signals of the oxide probably as a consequence of the formation of HCOO or CO_x species on the catalyst surface, but there was no indication of the presence of O vacancies. This is in contrast to results found for Cu/CeO_2(1 1 1) and Cu/TiO_2(1 1 0) [4,10], where the oxide support exhibits a significant concentration of O vacancies as a consequence of the WGS reaction. Due to the high ionicity of MgO, it is much more difficult to form O vacancies in this oxide than in CeO_2 or TiO_2 [34,35]. The oxygen vacancies present in Cu/CeO_2(1 1 1) and Cu/TiO_2(1 1 0) help in the dissociation of the water molecule and reduce the apparent activation energy for the WGS process [4,10,15]. Such a phenomenon cannot occur on the Cu/MgO(0 0 1) catalysts, and the main steps of the WGS probably take place on the Cu nanoparticles (notice the similarities in the apparent activation energies over Cu/MgO(0 0 1) and over a rough foil of copper). Thus, in the design of WGS catalysts, the reducibility of the oxide support is an important factor that must be taken into consideration. The kinetic data in Figs. 6 and 7 show, in a conclusive way, that in a good WGS catalyst the oxide is not a simple spectator and plays a direct role in the reaction process.

4. Conclusions

The water-gas shift reaction was studied on Cu(1 0 0), on a rough Cu foil, and on a series of Cu/MgO(1 0 0) surfaces (P_{CO} = 20 Torr; P_{H_2O} = 10 Torr; T = 575–650 K). An apparent activation energy of 13.8 kcal/mol was found for the Cu/MgO(1 0 0) catalyst. This is smaller than the value of 15.2 kcal/mol observed for Cu(1 0 0), but comparable to the value of 13.7 kcal/mol seen for a rough Cu foil. Post-reaction surface characterization pointed to the lack of O vacancies in the Cu/MgO(1 0 0) catalysts. This is in contrast to results found for Cu/CeO_2(1 1 1) and Cu/TiO_2(1 1 0), where the oxide support exhibits a significant concentration of O vacancies as a consequence of the WGS reaction. The oxygen vacancies present in Cu/CeO_2(1 1 1) and Cu/TiO_2(1 1 0) help in the dissociation of the water molecule and reduce the apparent activation energy for the WGS process to 7–9 kcal/mol. Such a phenomenon cannot occur on the Cu/MgO(0 0 1) catalysts, and the main steps of the WGS probably take place on the Cu nanoparticles. According to DFT calculations, the WGS activity of Cu nanoparticles is associated with their low-coordinated corner and edge sites, which make the nanoparticles more active than flat copper surfaces for breaking the O–H bonds of water.

Acknowledgement

The research carried out at Brookhaven National Laboratory was supported by the US Department of Energy (Chemical Sciences Division, DE-AC02-98CH10886). M. Pérez and J. Evans thank INTEVEP for a research grant that made possible part of this work.

References

[1] J.M. Thomas, W.J. Thomas, Principles and Practice of Heterogeneous Catalysis, VCH, New York, 1997.
[2] R. Tavares-Figueiredo, A.L. Dantas-Ramos, H. Martins-Carvalho, J.L.G. Fierro, Catal. Today 107–108 (2005) 671.
[3] Q. Fu, H. Saltsburg, M. Flytzani-Stephanopoulos, Science 301 (2003) 935.
[4] J.A. Rodriguez, P. Liu, J. Hrbek, J. Evans, M. Pérez, Angewandte Chemie Int. 46 (2007) 1329.
[5] R. Burch, Phys. Chem. Chem. Phys. 8 (2006) 5483.
[6] P. Liu, J.A. Rodriguez, J. Chem. Phys. 126 (2007) 164705.
[7] A.A. Gokhale, J.A. Dumesis, M. Mavrikakis, J. Am. Chem. Soc. 130 (2008) 1402.
[8] J. Nakamura, J.M. Campbell, C.T. Campbell, J. Chem. Soc., Faraday Trans. 86 (1990) 2725;
K.H. Ernst, C.T. Campbell, G. Moretti, J. Catal. 134 (1992) 66.
[9] J.A. Rodriguez, P. Liu, J. Hrbek, M. Pérez, J. Evans, J. Mol. Catal. A: Chem. 281 (2008) 59.
[10] J. Graciani, J. Evans, J.A. Rodriguez, J. Fernández-Sanz, Angewandte Chemie Int., submitted for publication.
[11] X. Wang, J.A. Rodriguez, J.C. Hanson, M. Perez, J. Evans, J. Chem. Phys. 123 (2005) 221101.
[12] W. Wen, L. Jing, M.G. White, N. Marinkovic, J.C. Hanson, J.A. Rodriguez, Catal. Lett. 113 (2007) 1.

[13] X. Wang, J.A. Rodriguez, J.C. Hanson, D. Gamarra, A. Martínez-Arias, M. Fernández-García, J. Phys. Chem. B 110 (2006) 428.
[14] C.V. Ovensen, P. Stoltze, J.K. Nørskov, C.T. Campbell, J. Catal. 134 (1992) 445.
[15] J.A. Rodriguez, S. Ma, P. Liu, J. Hrbek, J. Evans, M. Pérez, Science 318 (2007) 1757.
[16] I.D. Gonzalez, R.M. Navarro, M.C. Alvarez-Galván, F. Rosa, J.L.G. Fierro, Catal. Commun. 9 (2008) 1759.
[17] M.-C. Wu, C.M. Truong, D.W. Goodman, Phys. Rev. B 46 (1992) 12688.
[18] Z. Dohnálek, G.A. Kimmel, S.A. Joyce, P. Ayotte, R. Scott Smith, B.D. Kay, J. Phys. Chem. B 105 (2001) 3747.
[19] J.A. Rodriguez, T. Jirsak, S. Chaturvedi, J. Chem. Phys. 111 (1999) 8077.
[20] L. Barrio, P. Liu, J.A. Rodriguez, J.M. Campos-Martin, J.L.G. Fierro, J. Chem. Phys. 125 (2006) 164715.
[21] P. Liu, J.A. Rodriguez, J.T. Muckerman, J. Hrbek, Phys. Rev. B 67 (2003) 155416.
[22] C.T. Campbell, K. Daube, J. Catal. 104 (1987) 109.
[23] N. Schumacher, A. Boisen, S. Dahl, A.A. Gokhale, S. Kandoi, L.C. Grabow, J.A. Dumesic, M. Mavrikakis, I. Chorkendorff, J. Catal. 229 (2005) 265.
[24] C.V. Ovensen, B.S. Clausen, J. Schiøtz, P. Stoltze, H. Topsøe, J.K. Nørskov, J. Catal. 168 (1997) 133.
[25] S. Hilaire, X. Wang, T. Luo, R.J. Gorte, J. Appl. Catal. A 215 (2001) 271.
[26] Y. Li, Q. Fu, M. Flytzani-Stephanopoulos, Appl. Catal. B 27 (2000) 179.
[27] T. Shido, Y. Iwasawa, J. Catal. 141 (1993) 71.
[28] G. Jacobs, L. Williams, U. Graham, D. Sparks, B.H. Davis, J. Chem. Phys. B 107 (2003) 10398.
[29] I. Fishtik, R. Datta, Surf. Sci. 512 (2002) 229.
[30] N. Lopez, J.K. Nørskov, J. Am. Chem. Soc. 124 (2002) 11262.
[31] L. Barrio, P. Liu, J.A. Rodríguez, J.M. Campos-Martín, J.L.G. Fierro, J. Chem. Phys. 125 (2006) 164715.
[32] D. Tibiletti, F.C. Meunier, A. Goguet, D. Reid, R. Burch, M. Boaro, M. Vicario, A. Trovarelli, J. Catal. 244 (2006) 183.
[33] C.D. Wagner, W.M. Riggs, L.E. Davis, J.F. Moulder, G. Muilenberg, Handbook of X-ray Photoelectron Spectroscopy, Perkin-Elmer, Eden Praire, MN, 1977, pp. 82 and 104.
[34] J.A. Rodriguez, G. Liu, T. Jirsak, J. Hrbek, Z. Chang, J. Dvorak, A. Maiti, J. Am. Chem. Soc. 124 (2002) 5242.
[35] L. Giordano, G. Pacchioni, T. Bredow, J. Fernández-Sanz, Surf. Sci. 471 (2001) 21.